minerals

Occurrence and Composition of Columbite-(Fe) In the Reduced A-Type Desemborque Pluton, Graciosa Province (S-SE Brazil)

Astrid Siachoque *, Rodolfo Garcia and Silvio R.F. Vlach

Institute of Geosciences, Department of Mineralogy and Geotectonics, University of São Paulo,
05508-060 São Paulo, Brazil; pedrosogarcia@gmail.com (R.G.); srfvlach@usp.br (S.R.F.V.)

* Correspondence: astridsia1116@hotmail.com; Tel.: +55-11-943868028

Abstract: Columbite-(Fe) is a post-magmatic accessory mineral occurring within syenogranites and greisens from the Desemborque Pluton. The petrographic (SEM) and geochemical (EPMA and LA-ICPMS) examination of this mineral shows two distinct textural types within both the rocks, named columbite-1 and columbite-2. The columbite-1 type is characterized by zoned crystals with two stages of crystallization: i) An early Nb-rich cores with low Ta/(Ta + Nb) and Mn/(Mn + Fe) ratios (0.02–0.08 and 0.17 to 0.21 apfu, respectively), and ii) a later Ta-rich rims with higher Ta/(Ta + Nb) ratios (0.11–0.26) and similar Mn/(Mn + Fe) ratios (from 0.14 to 0.22) relative to the former cores. On the other hand, the columbite-2 type is defined by irregular crystals with patchy textures and very low Ta/(Ta + Nb) ratios (0.008–0.038) and moderate Mn/(Mn + Fe) ratios between 0.20 and 0.38. Trace element compositions of all columbite-(Fe) crystals are relatively enriched in HREEs and HFSEs; however, the columbite-2 presents higher abundances of REEs, Y, Th, U, Pb, Sc, and Sn relative to the columbite-1. This study highlights a unique hydrothermal origin for both the columbite types, but the textural relations of the columbite-2 crystals indicated that its formation is related to fluid-induced alterations of post-magmatic fluorite and/or cassiterite crystals at the final stage of the post-magmatic evolution.

Keywords: columbite-(Fe), A-type granites; greisens; hydrothermal processes; EPMA; LA-ICPMS

1. Introduction

Columbite is the main Nb-oxide in the orthorhombic columbite-tantalite group minerals (CGM) with the general formula AB_2O_6, where Fe^{2+} or Mn^{2+} occupies the A-site, and Nb^{5+} or Ta^{5+} the B-site [1,2]. End-members of this group are designated as columbite-(Fe), columbite-(Mn), tantalite-(Fe), and tantalite-(Mn) [3]. These minerals usually present a wide range of composition and structural variations including minor substitutions of Ti, Sn, W, Zr, Hf, Sc, and REEs (among others), which are related to cationic order-disorder phenomena between the A- and B-sites [4–8].

CGM are usually found in rare-metal granites and pegmatites [9–15] but these minerals are also common in F- and Li-rich peraluminous granitic systems and associated greisens [16–20]. The occurrence of CGM has attracted significant attention because they are minerals of economic interest hosted in several metallogenetic provinces worldwide [11]. In Brazil, CGM are reported in pegmatites from the Borborema Province [21–23], the Lourenço-Amapá Province, and the São Joao do Rei and Araçuaí districts [11], and also in the peralkaline Madeira granite from the Pitinga Mine [24].

This is the first report of columbite in reduced metaluminous to slightly-peraluminous granites and related greisens of the Desemborque Pluton from the A-type Graciosa Province in S-SE Brazil. In order to understand the genesis of the columbite occurrences in the studied rocks, we combined

detailed petrographic optical microscopy and scanning electron microscopy (SEM) textural examination together with chemical characterization using EPMA and LA-ICPMS techniques. This work also provides new data on major and trace element compositions of columbite in typical greisen rocks, which are very scarce in the literature.

2. The Desemborque Pluton

The Desemborque Pluton in the Guaraú Granite Massif [25] is one of the most interesting plutons from the Graciosa Province in S-SE Brazil (Figure 1). This province of A-type granites and syenites [26] is made up of several plutons and related volcanic and subvolcanic rocks emplaced at shallow crustal levels during a post-collisional extensional regime associated with the geodynamic evolution of the South-Southeastern part of the Gondwana area at 580 Ma [27,28]. The intrusions are grouped in two main petrographic associations: one is alkaline, including metaluminous and peralkaline alkali-feldspar granites and syenites, while the other aluminous, which is constituted by metaluminous to slightly-peraluminous syeno- and monzogranites [26,29].
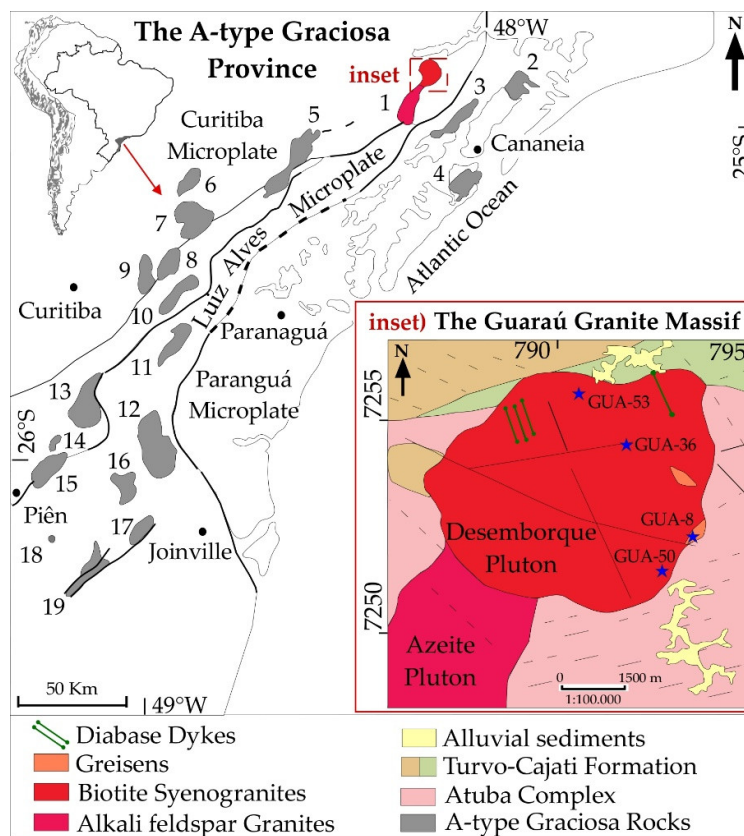

Figure 1. The location of the study area. The geological setting is of the Neoproterozoic A-type Graciosa province in S-SE Brazil (adapted from [26]). The A-type granites and syenites of the Graciosa Province are: (**1**) Guaraú Massif; (**2**) Serra do Paratiú/Cordeiro; (**3**) Mandira Massif; (**4**) Ilha do Cardoso; (**5**) Alto Turvo; (**6**) Capivari; (**7**) Órgãos; (**8**) Farinha Seca; (**9**) Anhangava; (**10**) Marumbi; (**11**) Serra da Igreja; (**12**) Morro Redondo Complex; (**13**) Palermo; (**14**) Agudos do Sul; (**15**) Rio Negro; (**16**) Dona Francisca; (**17**) Piraí; (**18**) Serra Alta; (**19**) Corupá; inset. A detailed geological map of the Guaraú Massif Granite, including the Desemborque and the Azeite plutons, is shown. The blue stars indicate the locations of columbite-bearing samples.

The Desemborque Pluton (Figure 1-inset) is a small subcircular intrusion (ca. 50 km²) in the Northeastern area of the province and intrudes the orthogneiss and metasedimentary sequences of the Atuba Complex and Turvo-Cajati Formation, respectively [30]. The pluton is relatively homogeneous and composed mainly of massive and/or porphyritic biotite syenogranites (Figure 2a,b),

and by alkali feldspar granites, granite porphyries, and microgranites, which are scarce [31]. Pegmatites and hydrothermal rocks resulting from the alteration of the main biotite syenogranites, such as greisenized granites and greisens [25,31], are also of local occurrence. Sampling of hydrothermally-altered rocks are difficult to see given the extensive weathering, thus greisenized granite and greisen rocks were sampled in a unique outcrop. This local well shows the contact relationships and the transition from the biotite syenogranite to the related greisen (Figure 2c,d). In the following, we focus our petrographic and geochemical descriptions of these rock varieties, and in Table 1 are listed their main geochemical compositions.
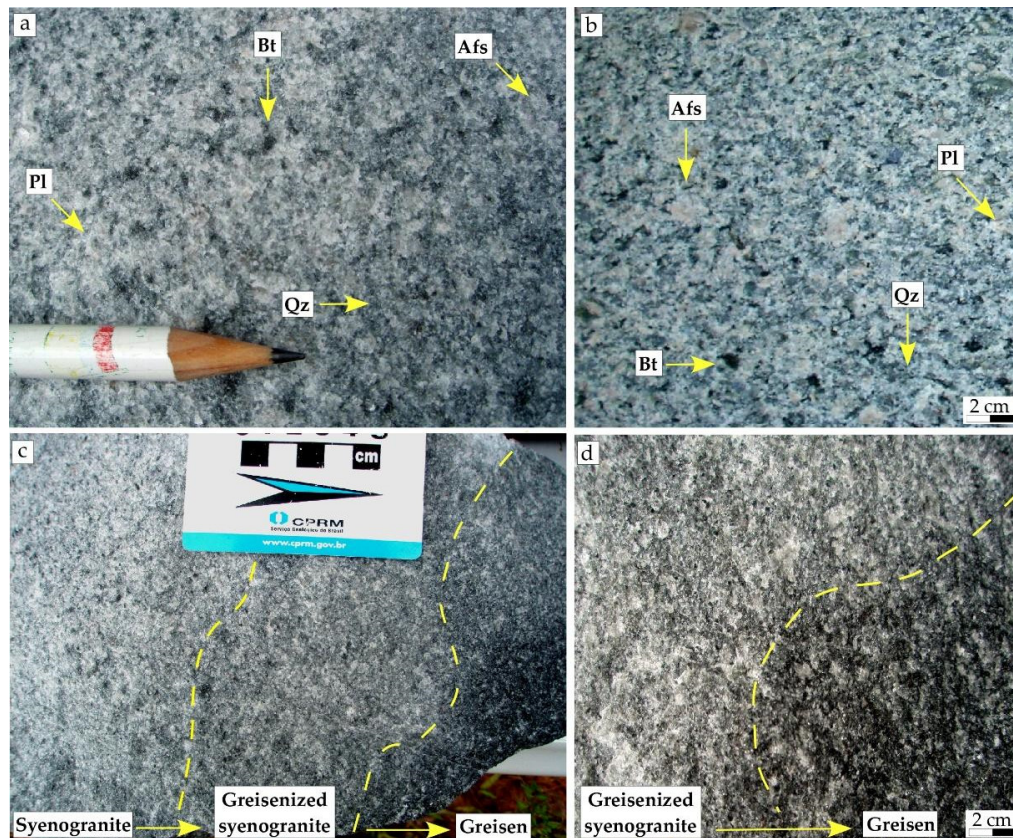

Figure 2. Macroscopic aspects of the Desemborque rocks. (**a**) Massive, fine-grained, leucocratic, grey-colored of the main syenogranite, showing equi- to inequigranular texture defined by quartz (Qz), plagioclase (Pl), and alkali feldspar crystals (Afs), as well as biotite (Bt) as the main mafic mineral; (**b**) porphyritic syenogranite showing rounded and/or tabular alkali feldspar in a fine-grained matrix of quartz, plagioclase, and interstitial biotite; (**c**) contacts between the main syenogranite with the greisenized granite and greisen rocks; (**d**) the detail of contact between greisenized syenogranite and greisen. Note the darker-colored aspect and the finer-grained texture of these rocks relative to the main biotite syenogranite.

2.1. The Biotite Syenogranite

The biotite syenogranite displays variably inequigranular medium- to coarse-grained and porphyritic textures (Figure 3a,b). It is composed of early-crystallized perthite orthoclase-(Or_{58-71}), oligoclase-albite (Ab_{78-95}), and quartz. Biotite, the only magmatic mafic phase among these rocks, varies in composition from annite to siderophyllite [31]. Zircon is the most abundant magmatic accessory mineral, followed by late-magmatic ilmenite and fluorite. Cassiterite, columbite, hematite, magnetite, monazite, and xenotime are common post-magmatic accessories, which are commonly included in aggregates of biotite. Other secondary and minor minerals are phengite, sericite, fluorides-HREE, and thorite are secondary minerals.

Geochemically, samples of this unit present average contents of 76.78 wt.% SiO_2, 12.18 wt.% Al_2O_3, 4.39 wt.% K_2O, 4.06 wt.% Na_2O and 1.07 wt.% Fe_2O_3, and a predominant metaluminous signature with A/CNK [molar ratio = $Al_2O_3/(CaO + Na_2O + K_2O)$] varying 0.96–0.99. They also show high Fe numbers [$Fe^* = FeO^T/(FeO^T + MgO)$, wt.% oxide] ~0.99, that contrast to other Graciosa granites within the aluminous association. Trace element compositions show a relatively high abundance of mainly F, Rb, Li and F (Table 1). Zircon U-Pb geochronological data point to crystallization ages of 580 ± 8 Ma [28].

2.2. Greisenized Syenogranite

The greisenized syenogranite is characterized by intermediate textural and chemical properties between the dominant syenogranite and the greisen. This rock presents an inequigranular fine-grained texture with post-magmatic transformations such as partial to complete replacement of feldspars by sericite and annite by zinnwaldite (Figure 3c). Other minerals found here are fluorite, ilmenite, hematite, phengite, and sphalerite. Geochemically, the greisenized syenogranite has intermediate compositions between the greisen and the hosted biotite syenogranite with relatively higher Fe_2O_3 and Al_2O_3 contents, and significant contents of F, Rb, Li, Y and Zr (Table 1).
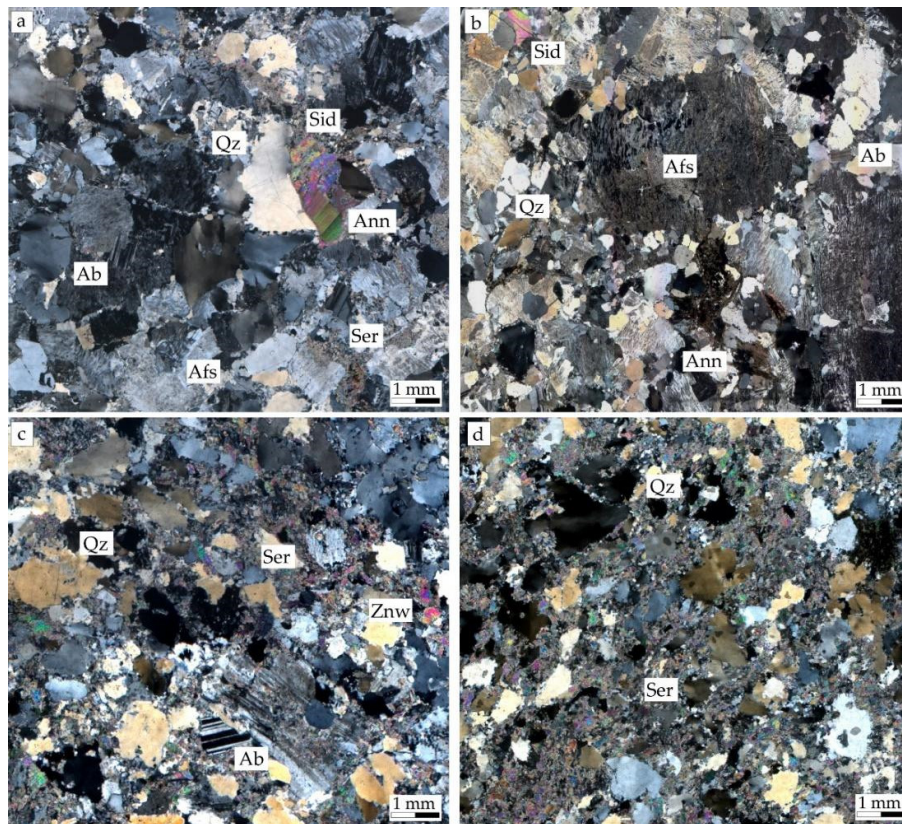

Figure 3. Microscopic aspects of the Desemborque studied rocks. (**a**) Syenogranite with equi- to inequigranular texture, including tabular perthitic alkali feldspar crystals (Afs), sometimes with albitic rims (Ab), as well as rounded and/or elongated quartz (Qz) with undulose extinction and interstitial annite (Ann) crystals. Note the partial alteration of some feldspars by sericite (Ser) and of the annite crystal by siderophyllite (Sid); (**b**) syenogranite with a porphyritic texture involving mesoperthitic alkali feldspars phenocryst in a medium-grained quartz-feldspar matrix; (**c**) greisenized syenogranite displaying inequigranular and altered texture and partial to complete replacement of feldspars by sericite and annite by zinnwaldite (Znw); (**d**) greisen characterized by heterogranoblastic texture with pervasive sericite-silica alteration, high recrystallization of quartz, and extensive replacement of zinnwaldite by sericite. Photomicrographs with crossed polarizers are shown.

2.3. Greisen

The studied sample is characterized by a fine-grained heterogranoblastic texture (Figure 3d), and its mineral assemblage is characterized by mainly quartz, accompanied by zinnwaldite-(Li) and sericite. Zircon, cassiterite, columbite, fluorite, monazite, thorite, and xenotime are the accessory minerals. Galena, sphalerite, and topaz are distinct accessories only found in this rock. Chemical compositions display a significant enrichment in Fe_2O_3, Li, Rb, Sn, Zr, and F and a discrete increase in Nb, Hf, Th, and U relative to the granite (Table 1).

Table 1. Chemical analyses for the studied Desemborque Rocks. Major (X-ray fluorescence spectrometry) and trace element (ICP-MS Inductively coupled plasma mass spectrometry).

Method	X-Ray Fluorescence			ICP-MS			
Samples	**GUA–50C**	**GUA–08a**	**GUA–08b**	**Samples**	**GUA–50C**	**GUA–08a**	**GUA–08b**
Unit	Syeno-granite	Greisenized syenogranite	Greisen	Unit	Syeno-granite	Greisenized syenogranite	Greisen
SiO_2 (wt%)	76.35	76.80	78.22	Li (ppm)	165	195	385
TiO_2	0.01	0.06	0.05	Be	6.2	5.6	6.6
Al_2O_3	12.26	12.64	10.13	Sn	6.0	46.1	116
Fe_2O_3	1.25	2.12	5.27	Sc	0.6	1.0	1.9
MnO	0.04	0.06	0.13	Rb	481	464	897
MgO	b.d.l	b.d.l	b.d.l	Sr	6.9	9.5	4.5
CaO	0.45	0.53	0.47	Y	212	164	159
Na_2O	3.91	3.78	0.26	Zr	82.3	116	156
K_2O	4.44	2.96	3.92	Nb	46.4	66.2	84.9
P_2O_5	0.01	0.00	0.00	Cs	4.2	10.0	31.6
LOI	0.62	0.98	1.48	Ba	51.7	4.1	4.3
Total	99.40	99.93	99.94	La	53.9	30.0	28.8
A/CNK	1.017	1.217	1.833	Ce	117	69.3	68.2
A.I	0.917	0.745	0.461	Pr	14.4	8.6	8.5
Fe*	0.996	0.997	0.999	Nd	55.7	32.2	32.2
Tsat(Zr)	746	-	-	Sm	16.9	10.2	10.4
CIPW norm				Eu	0.2	0.1	0.1
Q	35.21	-	-	Gd	20.3	11.9	12.2
C	0.22	-	-	Tb	4.2	2.7	2.7
Or	26.12	-	-	Dy	26.6	18.5	18.9
Ab	33.09	-	-	Ho	6.2	4.7	4.7
An	2.19	-	-	Er	17.9	14.7	14.4
Mt	1.81	-	-	Tm	2.9	2.6	2.5
Ilm	0.15	-	-	Yb	18.9	17.7	17.3
Ap	0.01	-	-	Lu	2.7	2.6	2.5
Ga (ppm)	25	31.6	35.7	Hf	4.9	8.3	11.0
Zn	58.1	62.3	62.3	Pb	36.9	20.5	13.5
Zr	92.9	142.8	153.3	Th	22.2	27.1	35.5
F	4624	6423	8999	U	4.6	7.3	13.6

LOI: lost on ignition; Fe* numbers; A/CNK: Alumina Saturation index; A.I: Agpaitic Index; Tsat(zr): temperature of zircon saturation; b.d.l: below detection limit.

Figure 4 shows the mineral assemblages at magmatic from late- to post-magmatic stages of evolution observed in the studied Desemborque rocks.
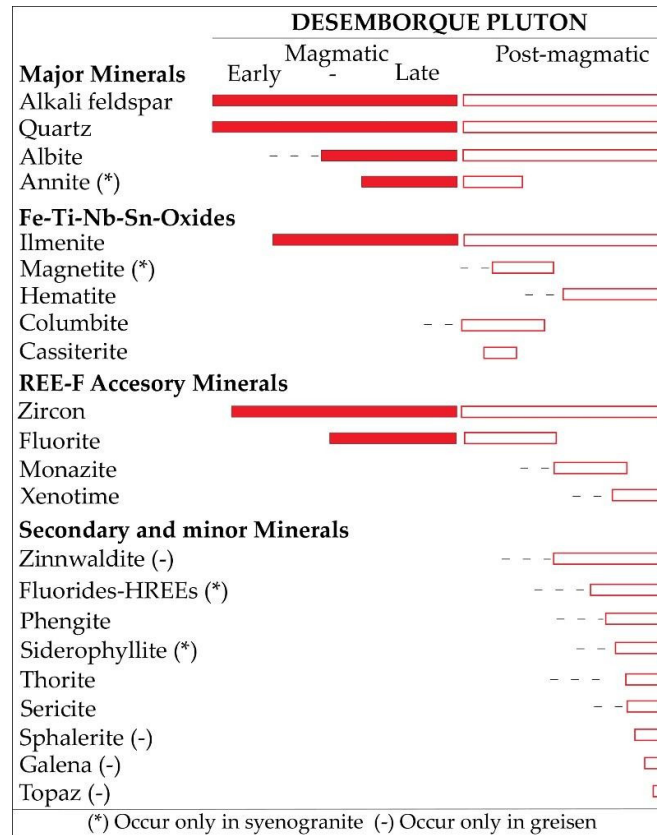
Figure 4. Interpreted crystallization sequence for the studied rocks from the Desemborque Pluton, showing the mineral occurrence at early-, late-, and post-magmatic stages.

3. Materials and Methods

Four samples bearing columbite crystals of the syenogranite (GUA−36, GUA−50, and GUA−53) and greisen (GUA−8b) varieties from the Desemborque Pluton were selected for petrographic, mineral chemistry, and whole-rock chemical data at the Laboratory of the NAP GeoAnalitica-Institute of Geosciences/University of São Paulo, Brazil.

Columbite crystals were identified in petrographic polished thin sections by combining optical and scanning electron microscopy (SEM) and semiquantitative energy dispersive spectrometry (EDS). Back-scattered electron images (BSE) were obtained to study internal textures and compositional variations. After textural descriptions, the chemical compositions of columbite crystals were determined using a JXA−8530 (JEOL, Tokyo, Japan) electron probe micro-analyzer (EPMA). A total of 42 analyses were conducted with an accelerating voltage of 20 kV, a beam current of 15 nA, a beam diameter of 3 μm, and maximum total peak-counting times, equally distributed between peak and background measures, varying between 5 s and 40 s. Standards used for analysis included diopside for Si, Ca, and Mg; ilmenite for Fe, Ti and Mn; anorthite for Al; albite for Na; zircon for Zr; fluorapatite for F; strontianite for Sr; yttrium-phosphate for Y; synthetic glasses for Gd and Th (all of them furnished by the Smithsonian Institute); and pure Pb, Sb, V, Ta, Nb and W metals (from the internal lab collection). Raw WDS data were corrected and converted to wt.% with the PRZ-Armstrong provided by JEOL. The detection limits for the conventional major oxides were in between 0.01 wt.% and 0.02 wt.%, and for the minor elements in between 0.02 wt.% and 0.26 wt.%. The structural formulae were calculated based on 6 oxygens and 3 atoms per formula unit (apfu).

Trace elements of columbite crystals were analyzed using a laser ablation system (LA-ICP.MS) with a 213 A/F equipment (New Wave, Portland, ME, USA). Analytical conditions were a laser spot of 25 μm, 20 Hz of frequency with an energy fluence of ~1.97 J/cm². Signal measurements and gas background on sample integration times were 60 and 40 s, respectively. The instrument was calibrated

with the NIST standard SRM 610 glass to correct signal drift during the analytical process and the basalt glass standard BCR−2G was used as an external standard to calibrate major and trace elements [32]. In Supplementary Table S2, the 2 sigma is reported.

Whole-rock chemical analyses were determined in three fresh samples (GUA−50c, GUA−08a, and GUA−08b) using an X-ray fluorescence instrument (XRF) with the Axios MAX Advanced equipment (PANalytical, Almelo, The Netherlands) and by Inductively coupled plasma mass spectrometry (ICP-MS) instrument with the iCAP Q ICP-MS equipment (Thermo Fisher Scientific, Bremen, Germany). Major and some minor elements were quantified by XRF, while trace elements and rare earth elements were measured by ICP-MS, following the analytical procedures developed by Reference [33] and Reference [34], respectively.

4. Results

4.1. Columbite Occurrence and Its Textural Relations

The examination of the petrographic thin sections of the biotite syenogranites and the greisen reveal that columbite occurs as individual or grouped opaque crystals. BSE images allowed the observation of two distinct textural types of columbite between both rocks types named columbite-1 and columbite-2, which present contrast modes of occurrence, internal textures, and compositional variations (Figure 5).
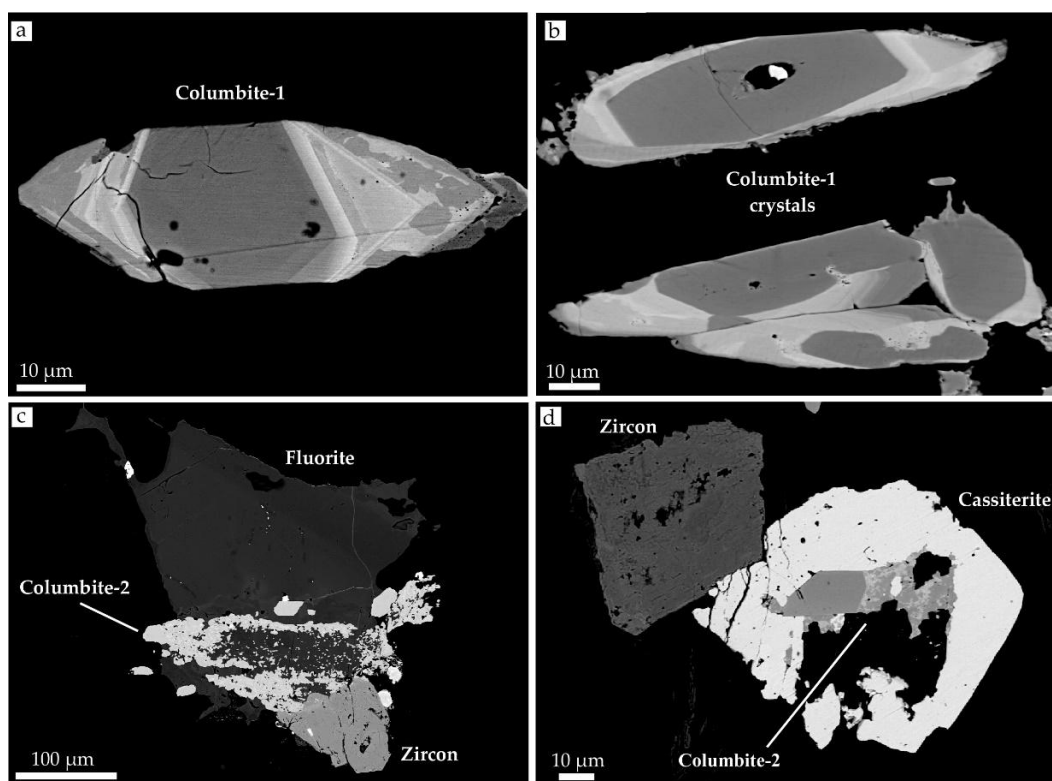

Figure 5. BSE images of columbite from the Desemborque Pluton showing the textural and compositional variations within crystals; (**a**) Euhedral columbite-1 crystal displaying convolute zoning with BSE-dark cores and BSE-bright and partially-spotted rims in syenogranite (Sample GUA−50C); (**b**) euhedral and subhedral columbite-1 grouped crystals showing zoning patterns with inward/irregular contact between the core and rim zones in the greisen (Sample GUA−08b). Of note, mostly crystals show partially corroded margins; (**c**) irregular intergrowths of columbite-2 replacing fluorite which occur in reaction texture with zircon in syenogranite (Sample GUA−53); (**d**) anhedral columbite-2 crystal with a patchy texture that occurs along cavities of cassiterite showing partial replacement of its crystals rims in syenogranite (Sample GUA−36).

The columbite-1 type is common in the greisen and rarely in the syenogranites. It occurs as subhedral to euhedral small (30–60 μm) prismatic crystals, displaying convolute zoning with BSE-dark cores and BSE-bright rims (Figure 5a,b). In syenogranites, columbite-1 crystals are partially fractured and display homogeneous cores and patchy domains within the rims (Figure 5a), whereas in the greisen the zoned patterns are irregularly distributed from the outer to the inner crystal parts (Figure 5b). The columbite-2 type is most common in the syenogranites and rarely found in the greisen; crystals are usually associated with fluorite, zircon and/or cassiterite and appear mostly as inclusions in biotite clusters within the syenogranites (Figure 5c,d). This type forms anhedral to subhedral crystals with variable shapes and sizes (up to 100 μm). They usually display resorption textures as partially dissolved domains, or domains with patchy areas and corroded margins, involving the partial replacement of fluorite (Figure 5c) and/or cassiterite (Figure 5d).

4.2. Mineral Chemistry

4.2.1. Main Features

Representative WDS chemical compositions and structural formulae for the identified columbite types are listed in Table 2; our complete EPMA data set is presented in Supplementary Table S1. In general, columbite-1 and -2 types in the Desemborque Pluton have equivalent compositions between syenogranites and the greisen. Comparing the data, all columbite crystals are Fe-rich and classified as columbite-(Fe) with Mn/(Mn + Fe) atomic ratios ranging from 0.14 to 0.22 for the columbite-1 type, and from 0.20 to 0.38 for the columbite-2 type; however, the Ta/(Ta + Nb) ratios show significant variability between both columbite types, especially within the columbite-1 zoned crystals (Figure 6). Thus, the cores of the columbite-1 crystals have Ta/(Ta + Nb) ratios from 0.02 to 0.08, while in the rims these ratios are always higher from 0.11 to 0.26. The EPMA results also reveal that columbite-1 crystals have relative higher apfu contents of W up to 0.092 (cores) and up to 0.080 (rims) as well as of Ti 0.093 (cores) and 0.110 (rims) when compared to the columbite-2 crystals up to 0.065 W and 0.089 Ti (Table S1). Moreover, the columbite-1 crystal rims present the highest contents of Zr (up to 0.010) and F (up to 0.014) between all columbite types (Table S1).

Table 2. Representative EPMA analysis of columbite crystals from the Desemborque Pluton.

| Sample	GUA−50C1			GUA−08			GUA−53		
Type	Columbite−1			Columbite−1			Columbite−2		
Point_ID	1-core	1a-rim	1b-rim	7-core	7a-rim	7b-rim	3-rim	4b-rim	4b-core
Rock type	Syenogranite			Greisen			Syenogranite		
SiO_2 (wt.%)	0.06	0.06	0.09	0.12	0.07	0.06	0.08	0.09	0.06
TiO_2	2.15	2.19	2.30	0.98	0.82	0.84	1.49	1.42	1.48
Al_2O_3	0.17	0.02	0.04	0.03	0.03	0.03	0.02	0.01	0.01
FeO	17.33	16.97	16.88	16.69	16.59	17.11	17.02	16.82	16.66
MnO	3.56	3.48	3.50	4.17	2.99	3.52	4.37	4.40	4.90
MgO	-	-	0.04	0.03	-	0.01	0.02	0.01	0.01
CaO	-	-	-	0.06	0.01	-	0.19	0.04	0.16
SrO	-	0.01	0.00	0.02	-	-	-	-	0.04
Sb_2O_5	0.04	-	-	-	-	0.01	-	-	-
V_2O_3	0.03	-	-	0.07	0.03	-	-	-	-
WO_3	4.11	3.90	4.18	1.76	1.41	1.80	1.72	1.51	0.92
ThO_2	-	0.02	0.04	0.01	0.02	0.03	-	-	0.02
UO_2	-	0.06	0.06	0.05	-	-	-	-	0.04
PbO	0.05	0.06	0.07	0.04	0.08	0.09	0.02	0.04	0.05
Na_2O	0.02	-	0.04	0.03	0.02	-	-	0.01	-
Gd_2O_3	0.03	-	0.04	-	0.01	0.02	0.09	0.00	0.00

Table 2. cont.

Sample	GUA−50C1			GUA−08			GUA−53		
Type	Columbite−1			Columbite−1			Columbite−2		
Point_ID	1-core	1a-rim	1b-rim	7-core	7a-rim	7b-rim	3-rim	4b-rim	4b-core
Rock type	Syenogranite			Greisen			Syenogranite		
Yb_2O_3	0.06	0.02	0.05	0.03	0.04	0.03	0.21	0.31	0.14
Y_2O_3	0.01	-	0.01	-	-	-	0.15	0.10	0.08
ZrO_2	0.27	0.21	0.30	0.16	0.11	0.05	0.21	0.16	0.09
Nb_2O_5	66.96	54.16	53.01	65.98	52.54	62.85	71.58	72.10	74.10
Ta_2O_5	4.96	18.76	19.15	9.05	24.61	14.41	1.93	2.21	0.98
F	0.06	0.05	-	-	-	-	0.35	0.00	0.02
Total	99.85	99.97	99.81	99.28	99.38	100.9	99.45	99.25	99.75
Structural formulae based on 3 cations and 6 oxygens									
W^{6+}	0.062	0.062	0.066	0.027	0.023	0.028	0.026	0.030	0.022
Nb	1.749	1.501	1.480	1.758	1.496	1.686	1.856	1.786	1.867
Ta	0.078	0.313	0.319	0.145	0.421	0.233	0.030	0.070	0.034
Ti	0.093	0.101	0.106	0.043	0.039	0.038	0.064	0.089	0.061
Zr	0.008	0.006	0.009	0.004	0.003	0.002	0.006	0.005	0.005
Sb^{5+}	0.001	-	-	-	-	-	-	0.001	-
V^{3+}	0.001	-	-	0.003	0.001	-	-	-	-
Y	-	-	-	-	-	-	0.005	0.001	0.003
Gd	0.001	0.000	0.001	-	-	-	0.002	-	-
Yb	0.001	-	0.001	0.001	0.001	0.001	0.004	0.001	0.005
Th	-	-	0.001	-	-	-	-	0.001	-
U	-	0.001	0.001	0.001	-	-	-	0.001	-
Pb	0.001	0.001	0.001	0.001	0.001	0.001	-	-	0.001
Si	0.003	0.004	0.005	0.007	0.004	0.004	0.004	0.008	0.005
Al	0.011	0.001	0.003	0.002	0.002	0.002	0.001	0.013	0.001
ΣB	2.009	1.991	1.993	1.992	1.993	1.995	1.999	2.006	2.014
Fe^{2+}	0.837	0.870	0.864	0.822	0.874	0.849	0.816	0.638	0.806
Mn	0.174	0.181	0.181	0.208	0.159	0.177	0.212	0.398	0.213
Mg	0.001	0.001	0.001	0.001	0.001	0.001	-	-	0.001
ΣA	1.012	1.052	1.047	1.031	1.035	1.027	1.029	1.036	1.020
#Mn	0.172	0.172	0.174	0.202	0.154	0.172	0.206	0.384	0.209
#Ta	0.043	0.172	0.177	0.076	0.220	0.121	0.016	0.037	0.018

#Mn: Mn/(Mn + Fe); #Ta: Ta/(Ta + Nb).
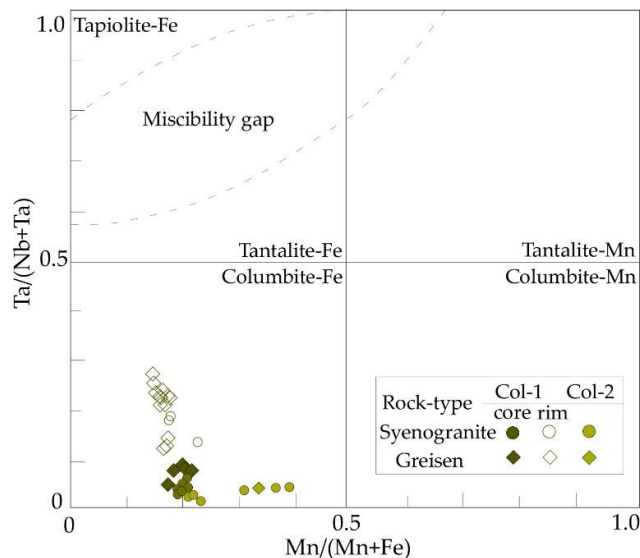
Figure 6. Columbite-group classification diagram with the Fe–Mn and Nb–Ta compositional variations for the columbite-crystals from the Desemborque Pluton.

The main chemical characteristics of the Desemborque columbite crystals are shown in Figure 7 and may be described by the compositional variations involving either single-site substitutions such Nb ↔ Ta and Mn ↔ Fe, or the coupled substitution represented by the following reaction:

$$2(V,Nb,Ta,Sb)^{5+} \leftrightarrow (Si,Ti,Zr,Th,U)^{4+} + (W)^{6+} \tag{1}$$
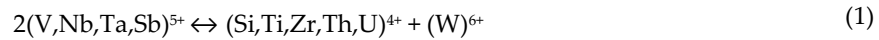
All cationic substitutions yield good correlations (determination coefficient r^2 in between 0.94 and 0.98). Compositional variations between the columbite types are, in general, limited to the columbite-1 zoned crystals which present a significant increase of Ta and somewhat of Fe from the core to the rims of compositions (Figure 7a,b). Nevertheless, the correlation between Mn and Fe shows that the columbite-2 crystals have rather larger variations (Figure 7b). Our data set also shows that both columbite-1 and -2 types indicate good balancing according to the coupled substitution scheme in Figure 7c, which gives the best correlation ($r^2 = 0.98$).
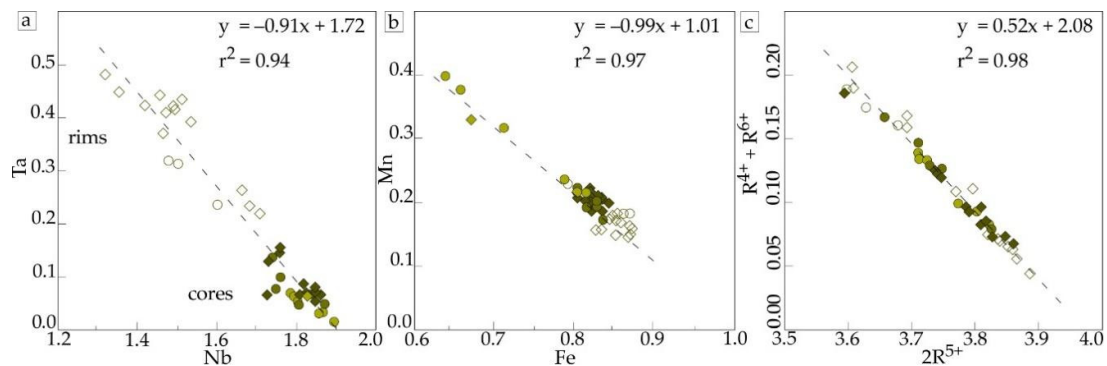

Figure 7. Compositional variations in columbite 1 and 2 crystals from the Desemborque Pluton. (**a**) Ta vs. Nb plot; (**b**) Mn vs. Fe plot; (**c**) $R^{4+} + R^{6+}$ vs. $2R^{5+}$ plot.

4.2.2. Trace and REE Element Compositions

Representative trace element analyses for the investigated columbite crystals are given in Table 3 and the complete dataset in Supplementary Table S2. Multielement and rare earth patterns are shown in Figure 8. Trace element patterns for columbite crystals exhibit some differences relative to those from the syenogranite and the greisen, especially the negative anomalies of Y and Th and the strong positive anomaly of U (Figure 8a). In general, columbite crystals are relatively enriched in most of the HREE and HFSE relative to corresponding whole-rock compositions.

The REE patterns for all columbite crystals show a rather steeply-rising slope due to the relative enrichment of HREE over the LREE ($28 < Yb_N/Ce_N < 3505$), with negative Eu anomalies [$Eu/Eu^* \cong Eu_N/(Sm_N*Gd_N)^{1/2}$] varying from 0.04 to 0.28 (Table S2). Comparing the columbite-1 and -2 crystals, the later present higher REE abundances ∑REE up to 3718 ppm, while the former register ∑REE up to 1362 ppm. The most contrasted REE pattern is observed in one columbite-2 crystal for the syenogranite, which has the highest REE abundances, especially the LREEs (1- to 2- fold higher than the others), with a contrasted LREE flatter pattern ($Sm_N/La_N \cong 1.38$).
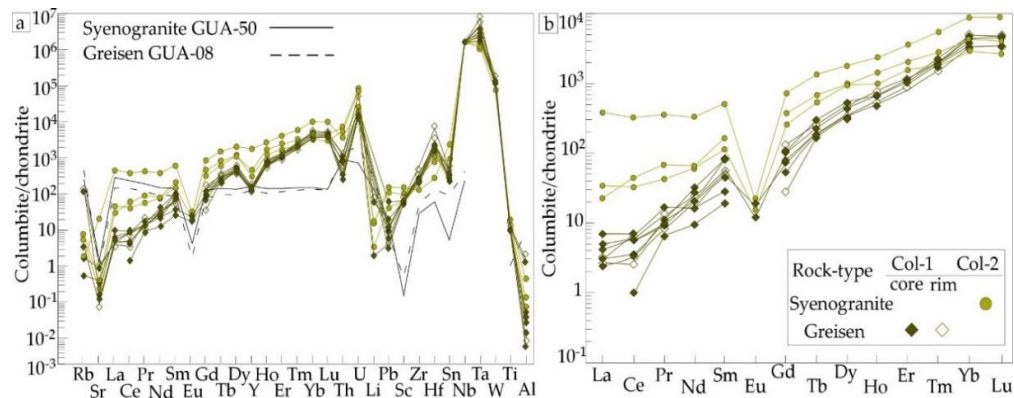
Figure 8. Chondrite normalized (**a**) trace element and (**b**) REE patterns for columbite crystals from the Desemborque Pluton. In the (**a**) diagram, the corresponding whole-rock patterns are also plotted. The data were normalized to the chondrite values of Reference [35].

Table 3. Representative LA-ICP-MS trace element analyses of the Desemborque columbite crystals.

Sample	GUA−08						GUA−53			
Rock	Greisen						Syenogranite			
Mineral	Columbite 1						Columbite 2			
Point	1-r	2σ	1-c	2σ	5-c	2σ	7-c	2σ	8-c	2σ
Li (ppm)	86.29	18	66.28	15	b.d.l	1.5	3.38	2.3	16.2	5.6
Sc	360	33	287.1	27	274	29	286	90	694	232
Ti	3860	333	3438	302	3279	353	3959	855	6443	1475
Rb	254	46	258	48	b.d.l	0.8	2.78	1.6	13.2	6.4
Sr	5.15	1.4	0.82	0.54	0.49	0.4	110	41	1.96	1.2
Y	203	16	174	14	160	14	2421	1184	397	207
Zr	1921	304	903	147	752	158	788	275	388	146
Sn	700	62	707	63	507	54	295	59	3340	694
La	0.72	0.6	1.68	0.8	0.62	0.4	90.6	38	8.17	4.1
Ce	3.87	1.2	4.01	1.3	1.95	0.7	196	68	20.2	8.2
Pr	0.83	0.6	1.00	0.6	b.d.l	0.4	32.7	14	4.03	2.2
Nd	11.01	8.1	14.55	9.6	9.11	7.9	147	27	27.2	13
Sm	7.86	4.6	12.06	5.8	7.04	3.8	78.1	13	17.9	7.9
Eu	b.d.l	0.6	b.d.l	0.7	0.93	0.9	1.35	1.2	0.77	1.2
Gd	26.08	8.0	20.02	7.1	14.44	5.1	144	67	51.4	28
Tb	9.46	2.2	8.17	2.0	6.81	1.9	48.6	20	19.3	9.0
Dy	117	23	106	22	82.25	21	443	244	238	142
Ho	42.23	5.4	37.9	5.0	26.65	3.8	128	57	55.3	26.4
Tb	9.46	2.2	8.17	2.0	6.81	1.9	48.6	20	19.3	9.0
Dy	117	23	106	22	82.25	21	443	244	238	142
Ho	42.23	5.4	37.9	5.0	26.65	3.8	128	57	55.3	26.4
Er	184	27	179	27	140	25	581	331	251	153
Dy	117	23	106	22	82.25	21	443	244	238	142
Ho	42.23	5.4	37.9	5.0	26.65	3.8	128	57	55.3	26.4
Er	184	27	179	27	140	25	581	331	251	153
Tm	51.51	8.7	58.1	9.8	40.6	8.5	134	33	46.4	13.1
Yb	796	172	690	152	522	145	1471	406	472	142
Lu	113	12	114	12.3	85.1	11	225	63	65.0	20
Hf	614	71	208	31	161	25	117	48	22.2	13
Pb	20.03	4.9	36.42	7.0	15.73	3.9	82.1	34	307	137
Th	30.25	4.6	16.71	3.1	6.07	1.5	90.5	35	149	62.1
U	409	60	167.3	26	89.22	18	175	89	492	266

b.d.l.: below detection limit; 2σ: 2 sigma error.

5. Discussion

5.1. Genesis of Columbite in the Desemborque Pluton

The explanation of the origin of columbite-group minerals (CGM) is always a challenge given the variable textures, alterations, and compositions recorded by these minerals during multiple stages of their crystallization. In granites, the formation of CGM have been extensively associated with magmatic and hydrothermal processes or a combination of both [16–20,36–41]. In this study, we suppose that the rare and local occurrence of columbite in the Desemborque pluton is indicative of a unique hydrothermal origin, as supported by the majority of columbite-1 crystals in the greisen and the replacement textures of columbite-2 crystals with other late- to post-magmatic accessory minerals in the syenogranites. However, the contrast of textural and geochemical features between the columbite-1 and -2 crystals suggest distinct mechanisms of formation.

In the case of columbite-1 group, zoning patterns within crystals indicate two hydrothermal substages of crystallization during the post-magmatic evolution: the first stage is represented by the formation of Nb-rich cores crystals, while the second stage is characterized by the subsequent crystallization of the Ta-rich rims around the former cores. These patterns are typical in CGM and have been broadly explained either by disequilibrium crystallization processes or differences in solubility, given the general tendency of Nb to crystallize prior to Ta during evolutionary stages [41–49]. Additionally, the somewhat higher abundances of the HFSEs (such Ti, Zr and Hf) of the Ta-rich rims crystals relative to the Nb-rich cores also suggest differentiated hydrothermal substages.

On the other hand, the formation of the columbite-2 crystals is interpreted as a result of dissolution-reprecipitation processes due to hydrothermal fluid-induced alterations at the final stage of the post-magmatic evolution. This can be explained by the disequilibrium textures, such as the resorption of the marginal and inner parts of fluorite and cassiterite shown in Figure 5c,d, which indicate that columbite-2 crystals formed as late replacements of these minerals. Moreover, the secondary patchy textures among the columbite-2 crystals reinforced the influence of post-magmatic hydrothermal fluids altering these crystals, which also could be responsible for the significant enrichment of REEs, Y, U, Th, Pb and Ti relative to the columbite-1 crystals.

5.2. Comparision with Other Columbite Occurrences from Rare-Granites And/Or Granitic Pegmatites Worldwide

In Figure 9, we compiled current compositional data of columbite-group minerals (colored lines) in granites and related greisens and used the previous schematic compilation of the #Ta and #Mn compositional evolution trends of columbite-group minerals from rare-metal granites worldwide (black lines) given by Reference [40] in order to compare with our results. The evolution trend of the columbite-1 crystals in the Desemborque Pluton is characterized by moderate variation of the Ta/(Ta + Nb) ratios (from 0.02 to 0.26), with a vertical trajectory that could be compared to those columbite trends from the Podlesí and Geyersberg Granites (Figure 9). The evolution trend of the Desemborque columbite-2 crystals shows a contrary horizontal and short trajectory, with limited variations of the Mn/(Mn + Fe) ratios (from 0.20 to 0.38), and differs from the others columbite trends compiled here.
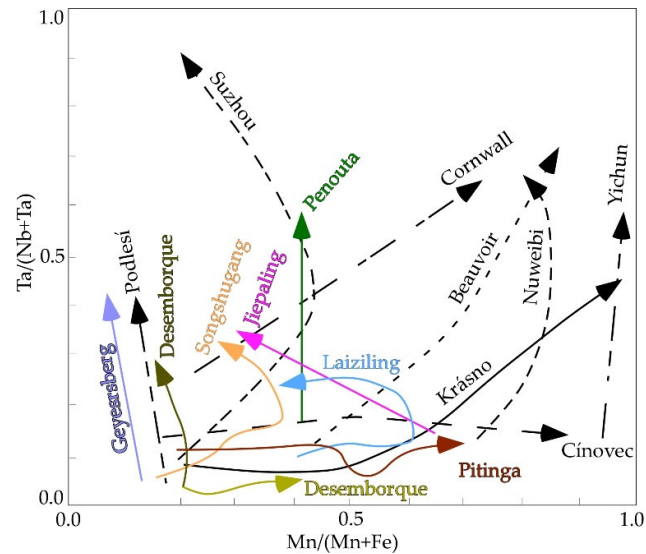
Figure 9. Compositional trends of columbite in F- and Li-rich rare-metal granitic systems and associated greisens worldwide after Reference [40]. Desemborque, South-Southern Brazil (this work); Geyersberg, Germany [20]; Laiziling, South China [38]; Penouta, Spain [18]; Jiepailing, South China [19]; Songshugang, Northeastern China [17]; Krásno, Germany [40]; Pitinga, North-Northwest Brazil [24]; Podlesí, Czech Republic [16]; Yichun, China [36]; Cínovec, Czech Republic [50]; Cornwall, England [51]; Suzhou, China [52]; Nuweibi, Egypt [53]; Beauvoir, France [54].

Detailed data on trace elements of CGM in granites and/or greisens are rarely found or absent in the literature. Nevertheless, a robust compilation of main and trace element compositions of CGM in typical pegmatites from relevant Ta–Nb–Sn provinces worldwide is provided by References [10,11]. We used the median trace element values of only columbite-(Fe) minerals from the mentioned dataset and plot with our average trace elements compositions, as shown in Figure 10. Trace element patterns of all the samples exhibit a clear LREE depleted and HREE enriched shape; U, Zr, Hf, and W are systematically enriched with respect to chondrite values, while Eu, Pb, Sn, Ti, Li, and Al are usually depleted. The behavior of elements such as Y, Th, and Sc are broadly variable among all columbite-(Fe) compositions, which can be attributed either to melt compositions and/or co-precipitation with other phases. For example, in the Desemborque Pluton, the negative anomalies of Y and Th for both columbite-1 and -2 crystals can be explained by the competition with xenotime within the hosting rocks. For the other examples presented here, we require further information on the mineral crystallization sequence from the hosting pegmatites which is far beyond the scope of this work. We also observed that our columbite-(Fe) compositions have much higher trace element abundances, especially for the LRREs, than the majority of the columbite occurrences worldwide (Figure 10).
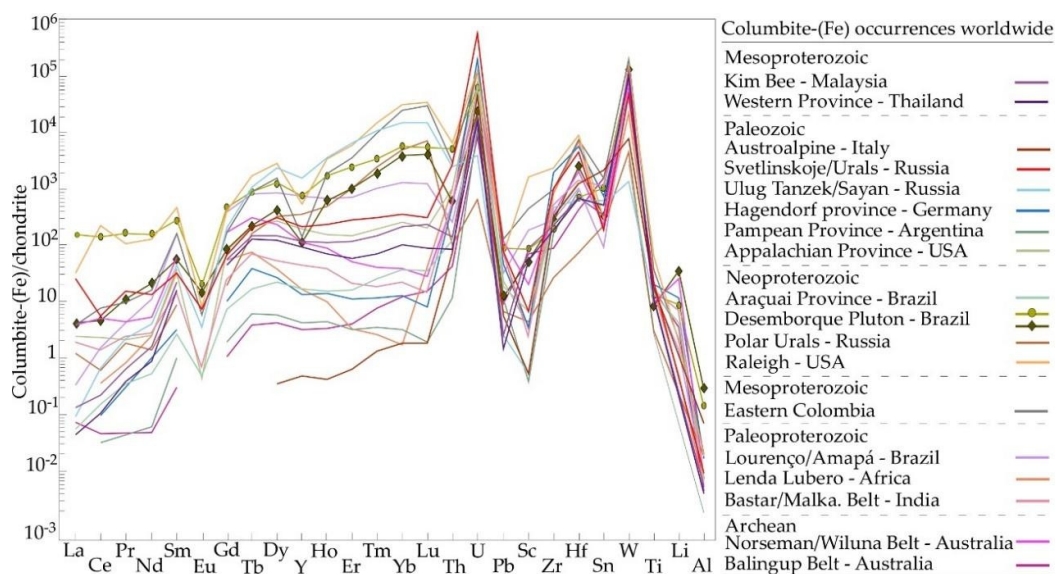
Figure 10. Average chondrite normalized rare-earth and trace element patterns for the studied columbite-(Fe) occurrences from the Desemborque Pluton, Brazil, and from pegmatites from worldwide provinces compiled by References [10,11].

6. Conclusions

Petrographic examination and geochemical data for columbite-(Fe) in syenogranites and related greisen from the reduced A-type Desemborque Pluton in the Graciosa Province (S-SE Brazil) indicate that the occurrence of columbite in the studied rocks is mainly associated with hydrothermal origin during the post-magmatic stage of crystallization. Textural and compositional variations of this mineral reveal two main textural types, named columbite-1 and columbite-2, which are interpreted as being formed by distinct mechanisms of crystallization. The columbite-1 is characterized by zoned crystals, which record two hydrothermal stages of crystallization: an early Nb-rich core, and then later Ta-rich rims. In contrast, columbite-2 is defined by irregular crystals with patchy textures, and its formation is related to disequilibrium processes driven by fluid-induced hydrothermal alterations involving the partial replacement of fluorite and/or cassiterite at the final post-magmatic stage.

The main chemical features of columbite types show that the columbite-1 crystals form an evolution trend with a significant increase of Ta/Nb ratios, while the columbite-2 crystals show a distinct trend with a limited increase of Mn/Fe ratios. Additionally, trace element compositions show that all columbite crystals are relatively enriched in HREEs and HFSEs; however, the columbite-2 type presents higher abundances of REEs, Y, Th, U, Pb, Sc, and Sn relative to the columbite-1 crystals. The chemical contrasts among the columbite types are related to disequilibrium crystallization processes (columbite-1) and to hydrothermal alterations during the post-magmatic evolution (columbite-2).

References

1. Ercit, T.S. The geochemistry and crystal chemistry of columbite-group minerals from granitic pegmatites, southwestern Grenville Province, Canadian Shield. *Can. Mineral.* **1994**, *32*, 421–438.

2. Černý, P.; Ercit, T.S. Mineralogy of Niobium and Tantalum: Crystal Chemical Relationships, Paragenetic Aspects and Their Economic Implications. In *Lanthanides, Tantalum and Niobium*; Möller, P., Černý, P., Saupé, F., Eds.; Springer: Berlin/Heidelberg, Germany, 1989; pp. 27–79.

3. Burke, E.A.J. Tidying up mineral names: An IMA-CNMNC scheme for suffixes, hyphens and diacritical marks. *Mineral. Rec.* **2008**, *39*, 131–135.

4. Černý, P.; Turnock, A.. Niobium-Tantalum minerals from granitic pegmatites at Greer Lake, Southeastern Manitoba. *Can. Mineral.* **1971**, *10*, 755–772.

5. Černý, P.; Ercit, T.S. Some recent advances in the mineralogy and geochemistry of Nb and Ta in rare-element granitic pegmatites. *Bull. Minéralogie* **1985**, *108*, 499–532.

6. Wenger, M.; Armbruster, T.; Geiger, C.A. Cation distribution in partially ordered columbite from the Kings Mountain pegmatite, North Carolina. *Am. Mineral.* **1991**, *76*, 1897–1904.

7. Ercit, T.S.; Wise, M.A.; Černy, P. Compositional and structural systematics of the columbite group. *Am. Mineral.* **1995**, *80*, 613–619.

8. Černý, P.; Ercit, T.S.; Wise, M.A.; Chapman, R.; Buck, H.M. Compositional, structural and phase relationships in titanian ixiolite and titanian columbite-tantalite. *Can. Mineral.* **1998**, *36*, 547–561.

9. Tindle, A.G.; Breaks, F.W. Columbite-tantalite mineral chemistry from rare-element granitic pegmatites: Separation Lake area, N.W. Ontario, Canada. *Mineral. Petrol.* **2000**, *70*, 165–198.

10. Melcher, F.; Graupner, T.; Gäbler, H.E.; Sitnikova, M.; Henjes-Kunst, F.; Oberthür, T.; Gerdes, A.; Dewaele, S. Tantalum-(niobium-tin) mineralisation in African pegmatites and rare metal granites: Constraints from Ta-Nb oxide mineralogy, geochemistry and U-Pb geochronology. *Ore Geol. Rev.* **2015**, *64*, 667–719.

11. Melcher, F.; Graupner, T.; Gäbler, H.-E.; Sitnikova, M.; Oberthür, T.; Gerdes, A.; Badanina, E.; Chudy, T. Mineralogical and chemical evolution of tantalum–(niobium–tin) mineralisation in pegmatites and granites. Part 2: Worldwide examples (excluding Africa) and an overview of global metallogenetic patterns. *Ore Geol. Rev.* **2016**, *89*, 946–987.

12. Badanina, E.V.; Sitnikova, M.A.; Gordienko, V.V.; Melcher, F.; Gäbler, H.E.; Lodziak, J.; Syritso, L.F. Mineral chemistry of columbite-tantalite from spodumene pegmatites of Kolmozero, Kola Peninsula (Russia). *Ore Geol. Rev.* **2015**, *64*, 720–735.

13. Van Lichtervelde, M.; Salvi, S.; Beziat, D.; Linnen, R.L. Textural features and chemical evolution in tantalum oxides: Magmatic versus hydrothermal origins for Ta mineralization in the Tanco Lower pegmatite, Manitoba, Canada. *Econ. Geol.* **2007**, *102*, 257–276.

14. Melcher, F.; Graupner, T.; Oberthur, T.; Schutte, P. Tantalum-(niobium-tin) mineralisation in pegmatites and rare-metal granites of Africa. *South African J. Geol.* **2017**, *120*, 77–100.

15. Černý, P.; Goad, B.E.; Hawthorne, F.C.; Chapman, R. Fractionation trends of the Nb- and Ta-bearing oxide minerals in the Greer Lake pegmatitic granite and its pegmatite aureole, southeastern Manitoba. *Am. Mineral.* **1986**, *71*, 501–517.

16. Breiter, K.; Škoda, R.; Uher, P. Nb-Ta-Ti-W-Sn-oxide minerals as indicators of a peraluminous P- and F-rich granitic system evolution: Podlesí, Czech Republic. *Mineral. Petrol.* **2007**, *91*, 225–248.

17. Zhu, Z.Y.; Wang, R.C.; Che, X.D.; Zhu, J.C.; Wei, X.L.; Huang, X. Magmatic-hydrothermal rare-element mineralization in the Songshugang granite (northeastern Jiangxi, China): Insights from an electron-microprobe study of Nb-Ta-Zr minerals. *Ore Geol. Rev.* **2015**, *65*, 749–760.

18. Llorens González, T.; Moro Benito, M.C.; Sanz Contreras, J.L.; López Moro, F.J.; García Polonio, F.; Fernández Fernández, A. Tin-tantalum-niobium mineralization in the Penouta deposit (NW Spain): Textural features and mineral chemistry to unravel the genesis and evolution of cassiterite and columbite group minerals in a peraluminous system. *Ore Geol. Rev.* **2016**, *81*, 79–95.

19. Xie, L.; Wang, R.-C.; Che, X.-D.; Huang, F.-F.; Erdmann, S.; Zhang, W.-L. Tracking magmatic and hydrothermal Nb–Ta–W–Sn fractionation using mineral textures and composition: A case study from the late Cretaceous Jiepailing ore district in the Nanling Range in South China. *Ore Geol. Rev.* **2016**, *78*, 300–321.

20. René, M. Nb-Ta-Ti oxides in topaz granites of the Geyer granite stock (Erzgebirge Mts., Germany). *Minerals* **2019**, *9*, 14.

21. Baumgartner, R.; Romer, R.L.; Moritz, R.; Sallet, R.; Chiaradia, M. Columbite–Tantalite-Bearing Granitic Pegmatites from the Seridó Belt, Northeastern Brazil: Genetic constrains from U–Pb dating and Pb isotopes. *Can. Mineral.* **2006**, *44*, 69–86.

22. Beurlen, H.; Soares, D.R.; Thomas, R.; Prado-Borges, L.E.; De Castro, C. Mineral chemistry of tantalate species new in the Borborema Pegmatitic Province, Northeast Brazil. *An. Acad. Bras. Cienc.* **2005**, *77*, 169–182.

23. Beurlen, H.; Da Silva, M.R.R.; Thomas, R.; Soares, D.R.; Olivier, P. Nb–Ta–(Ti–Sn) oxide mineral chemistry as tracer of rare-element granitic pegmatite fractionation in the Borborema Province, Northeastern Brazil. *Miner. Depos.* **2007**, *43*, 207–228.

24. Bastos Neto, A.C.; Pereira, V.P.; Ronchi, L.H.; De Lima, E.F.; Frantz, J.C. The world-class Sn, Nb, Ta, F (Y, REE, Li) deposit and the massive cryolite associated with the albite-enriched facies of the madeira A-type granite, Pitinga Mining District, Amazonas State, Brazil. *Can. Mineral.* **2009**, *47*, 1329–1357.

25. Oliveira, M.C.B.; Rodrigues, E. de P.; Coutinho, J.M.V.; Martins, F.A.G.; Figueiredo, M.C.H. de F.; Zaparolli, L.H. Petrologia de parte do Maciço granítico Guarau-SP. Atas. In Proceedings of the III Simpósio Sul-Brasileiro Geologia; Curitiba. Brazil, 5–10 November 1987; pp. 571–594.

26. Gualda, G.A.R.; Vlach, S.R.F. The Serra da Graciosa A-type granites and syenites, southern Brazil. Part 1: Regional setting and geological characterization. *An. Acad. Bras. Cienc.* **2007**, *79*, 405–430.

27. Vlach, S.R.F.; Siga, O.; Harara, O.M.M.; Gualda, G. a R.; Basei, M. a S.; Vilalva, F.C.J. Crystallization ages of the A-type magmatism of the Graciosa Province (Southern Brazil): Constraints from zircon U-Pb (ID-TIMS) dating of coeval K-rich gabbro-dioritic rocks. *J. South Am. Earth Sci.* **2011**, *32*, 407–415.

28. Vilalva, F.C.J.; Simonetti, A.; Vlach, S.R.F. Insights on the origin of the Graciosa A-type granites and syenites (Southern Brazil) from zircon U-Pb geochronology, chemistry, and Hf and O isotope compositions. *Lithos* **2019**, *340–341*, 20–33.

29. Gualda, G.A.R.; Vlach, S.R.F. The Serra da Graciosa A-type Granites and Syenites, southern Brazil. Part 2: Petrographic and mineralogical evolution of the alkaline and aluminous associations. *Lithos* **2007**, *93*, 310–327.

30. Faleiros, F.M.; Campanha, G.A. da C.; Martins, L.; Vlach, S.R.F.; Vasconcelos, P.M. Ediacaran high-pressure collision metamorphism and tectonics of the southern Ribeira Belt (SE Brazil): Evidence for terrane accretion and dispersion during Gondwana assembly. *Precambrian Res.* **2011**, *189*, 263–291.

31. Garcia, R.P. Evolução Magmática e Hidrotermal de Granitos de "Tipo-A" Reduzidos: O Exemplo do Pluton Desemborque, Maciço Guaraú, SP. Master's Thesis, Universty of São Paulo, São Paulo, Brazil, 2015.

32. Jochum, K.P.; Weis, U.; Stoll, B.; Kuzmin, D.; Yang, Q.; Raczek, I.; Jacob, D.E.; Stracke, A.; Birbaum, K.; Frick, D.A.; et al. Determination of reference values for NIST SRM 610-617 glasses following ISO guidelines. *Geostand. Geoanalytical Res.* **2011**, *35*, 397–429.

33. Mori, P.E.; Reeves, S.; Correia, C.T.; Haukka, M. Development oof a fused glass disc XRF facility and comparison with the pressed powder pellet technique at Instituto de Geociencias, Sao Paulo University. *Rev. Bras. Geociencias* **1999**, *29*, 441–446.

34. Navarro, M.S.; Andrade, S.; Ulbrich, H.; Gomes, C.B.; Girardi, V.A.V. The direct determination of rare earth elements in basaltic and related rocks using ICP-MS: Testing the efficiency of microwave oven sample decomposition procedures. *Geostand. Geoanalytical Res.* **2008**, *32*, 167–180.

35. McDonough, W.F.; Sun, S. The composition of the Earth. *Chem. Geol.* **1995**, *120*, 223–253.

36. Belkasmi, M.; Cuney, M.; Pollard, P.J.; Bastoul, A. Chemistry of the Ta-Nb-Sn-W oxide minerals from the Yichun rare metal granite (SE China): Genetic implications and comparison with Moroccan and French Hercynian examples. *Mineral. Mag.* **2000**, *64*, 507–523.

37. Huang, X.L.; Wang, R.C.; Hu, H.; Chen, X.M.; Liu, C.S. Vertical Variations in the Mineralogy of the Yichun Topaz Lepidolite Granite, Jiangxi Province, Southern China. *Can. Mineral.* **2002**, *40*, 1047–1068.

38. Xie, L.; Wang, Z.; Wang, R.-C.; Zhu, J.C.; Che, X.; Gao, J.; Zhao, X. Mineralogical constraints on the genesis of W-Nb-Ta mineralization in the Laiziling granite (Xianghualing distric, sout China). *Ore Geol. Rev.* **2018**, *95*, 695–712.

39. Alfonso, P.; Hamid, S.A.; Garcia-Valles, M.; Llorens, T.; López Moro, F.J.; Tomasa, O.; Calvo, D.; Guasch, E.; Anticoi, H.; Oliva, J.; et al. Textural and mineral-chemistry constraints on columbite-group minerals in the Penouta deposit: Evidence from magmatic and fluid-related processes. *Mineral. Mag.* **2018**, *82*, S199–S222.

40. René, M.; Škoda, R. Nb-Ta-Ti oxides fractionation in rare-metal granites: Krásno-Horní Slavkov ore district, Czech Republic. *Mineral. Petrol.* **2011**, *103*, 37–48.

41. Ballouard, C.; Poujol, M.; Boulvais, P.; Branquet, Y.; Tartèse, R.; Vigneresse, J.L. Nb-Ta fractionation in peraluminous granites: A marker of the magmatic-hydrothermal transition. *Geology* **2016**, *44*, 231–234.

42. Linnen, R.L.; Keppler, H. Columbite solubility in granitic melts: Consequences for the enrichment and fractionation of Nb and Ta in the Earth's crust. *Contrib. Mineral. Petrol.* **1997**, *128*, 213–227.

43. Linnen, R.L. The solubility of Nb-Ta-Zr-Hf-W in granitic melts with Li and Li + F: Constraints for mineralization in rare metal granites and pegmatites. *Econ. Geol.* **1998**, *93*, 1013–1025.

44. Linnen, R.L.; Cuney, M. Granite-related rare-element deposits and experimental constraints on Ta-Nb-W-Sn-Zr-Hf mineralization. In *Rare Element Geochemistry and Mineral Deposits;* Linnen, R.L., Samson, I.M., Eds.; Short Course Notes; Geological Association of Canada: St. Jonh's, NL, Canada, 2005; Volume 17, pp. 45-68.

45. Zaraisky, G.P.; Korzhinskaya, V.; Kotova, N. Experimental studies of Ta2O5 and columbite-tantalite solubility in fluoride solutions from 300 to 550 °C and 50 to 100 MPa. *Mineral. Petrol.* **2010**, *99*, 287–300.

46. Chevychelov, V.Y.; Borodulin, G.P.; Zaraisky, G.P. Solubility of columbite, (Mn, Fe)(Nb, Ta)2O6, in granitoid and alkaline melts at 650–850 °C and 30–400 MPa: An experimental investigation. *Geochem. Int.* **2010**, *48*, 456–464.

47. Chevychelov, V.Y.; Zaraisky, G.P.; Borisovskii, S.E.; Borkov, D.A. Effect of melt composition and temperature on the partitioning of Ta, Nb, Mn, and F between granitic (alkaline) melt and fluorine-bearing aqueous fluid: Fractionation of Ta and Nb and conditions of ore formation in rare-metal granites. *Petrology* **2005**, *13*, 305–321.

48. Stepanov, A.S.; Meffre, S.; Mavrogenes, J.; Steadman, J. Nb-Ta fractionation in peraluminous granites: A marker of the magmatichydrothermal transition. *Geology* **2016**, *44*, e394.

49. Ballouard, C.; Branquet, Y.; Tartèse, R.; Poujol, M.; Boulvais, P.; Vigneresse, J. Nb-Ta fractionation in peraluminous granites: A marker of the magmatic-hydrothermal transition: REPLY. *Geology* **2016**, *44*, e395–e395.

50. Rub, A.K.; Štemprok, M.; Rub, M.G. Tantalum mineralization in the apical part of the Cínovec (Zinnwald) granite stock. *Mineral. Petrol.* **1998**, *63*, 199–222.

51. Scott, P.W.; Pascoe, R.D.; Hart, F.W. Columbite-tantalite, rutile and other accessory minerals from the St. Austell topaz granite, Cornwall. *Proc. Usher Soc.* **1998**, *9*, 165–170.

52. Wang, R.C.; Fontan, F.; Xu, S.J.; Chen, X.M.; Monchoux, P. The association of columbite, tantalite and tapiolite in the Suzhou Granite, China. *Can. Mineral.* **1997**, *35*, 699–706.

53. Abdalla, H.M.; Helba, H..; Mohamed, F.. Chemistry of columbite-tantalite minerals in rare metal granitoids, Easterns Desert, Egypt. *Mineral. Mag.* **1998**, *62*, 821–836.

54. Wang, R. *Étude Minéralogique et Cristallochimique de Cassitérite, Niobo-tantalates et Minéraux Disséminés du Granite de Beauvoir (Allier); Implications Métallogéniques*; Paul Sabatier: Toulouse, France, 1998.